

HEAT TRANSFER ON THE MIDDLE GENERATRIX OF A  
HORIZONTAL PIPE IN THE TURBULENT FLOW OF  
LOW-TEMPERATURE HELIUM

M. A. Valyuzhinich, S. N. Vostrikov,  
V. M. Eroshenko, E. V. Kuznetsov,  
and O. A. Shevchenko

UDC 536.24:521.59

Results are presented from an experimental study of heat transfer in a turbulent helium flow under conditions of forced and mixed convection in horizontal pipes.

The cooling of several types of power equipment with low-temperature helium involves the use of heat exchangers with horizontal channels. The helium flow may become layered across the channel as a result of thermogravitational forces and the appearance of secondary flows. It should be noted that experimental studies of heat exchange in the flow of supercritical helium have been performed mainly on vertical pipes [1-6], with the effect of thermogravitational forces being weak. Only recently have several works been published [7-12] which presented results of tests of helium flows in horizontal pipes. In [7-10] the cooling regimes corresponded to conditions in which the thermogravitational effect was slight. With an increase in the thermal load, investigators [7] noted the onset of temperature fluctuations on the pressure wall. Experimental studies of heat exchange in a helium flow characterized by mixed convection [11, 12] showed that heat transfer differed significantly on the upper and lower generatrices of a horizontal pipe: heat transfer decreased on the upper generatrix and increased on the lower generatrix with an increase in thermal load.

Here there arises the question as to the ratio of heat transfer on the sections between the upper and lower pipe generatrices in the cases of mixed and forced convection. It may be suggested that the heat-transfer coefficients are equal on a section near the middle generatrix of the pipe. This problem is also methodologically important in connection with the need to properly install temperature transducers on the wall of horizontal channels of small diameter.

The present work attempts to determine heat transfer on the middle generatrix of horizontal pipes of different diameters within a broad range of Gr numbers and to compare the data with well-known empirical data on vertical pipes, when there is no layering of the coolant across the channel and the flow regime is close to forced convection. One of the problems encountered also is comparing test data on the middle generatrix with theoretical values found from correlation equations (1) [13] and [14], which adequately generalize test data on heat transfer to helium [1, 2, 4] with boundary conditions of the second type and forced convection in normal, "deteriorated," and "improved" heat-transfer regimes:

$$\frac{\text{Nu}}{\text{Nu}_0} = \frac{(T_w/\bar{T})^{-0.5}}{m + (1-m) \frac{c_p(T_w - \bar{T})}{H_w - \bar{H}} + 0.4 \exp\left(1 - \frac{T_w}{T^*}\right) \beta(T_w - \bar{T}) \text{Pr}^{-0.6} \left(\frac{T_w}{\bar{T}}\right)^{-0.5}}, \quad (1)$$

where  $m = 0.5$ .

Such a comparison was made for pipe sections with stabilized thermal and hydrodynamic characteristics. We assumed that thermal stabilization for horizontal pipes in a regime of mixed convection begins at a distance greater than  $x/d = 50$  from the beginning of the pipe heating section.

The tests were conducted in horizontal stainless-steel pipes of large and small diameter.

G. M. Krzhizhanovskii State Scientific-Research Energy Institute, Moscow. Translated from *Inzhenerno-Fizicheskii Zhurnal*, Vol. 46, No. 3, pp. 357-362, March, 1984. Original article submitted January 27, 1983.

TABLE 1. Regime Parameters and Test Data ( $d_e = 18$  mm)

| No. | $10^{-5} P, \text{ N/m}^2$ | $10^3 G, \text{ kg/sec}$ | $q_w, \text{ W/m}^2$ | $T_0, \text{ K}$ | A. SI units | $\frac{T_w}{\varphi=\pi/2}, \text{ K}$ | $\frac{Nu}{\varphi=\pi/2}$ |
|-----|----------------------------|--------------------------|----------------------|------------------|-------------|--|----------------------------|
| 1   | 0,120                      | 0,52                     | 169,1                | 15               | 42,8        | 26,36                                  | 0,71                       |
| 2   | 0,178                      | 1,08                     | 384,1                | 6,5              | 34,2        | 19,89                                  | 0,76                       |
| 3   | 0,248                      | 1,08                     | 383,2                | 6,8              | 55,1        | 20,11                                  | 0,79                       |
| 4   | 0,13                       | 0,26                     | 176,4                | 13,2             | 79,1        | 33,4                                   | 0,89                       |
| 5   | 0,113                      | 0,24                     | 117,6                | 24,96            | 56,3        | 41,5                                   | 0,61                       |
| 6   | 0,165                      | 4,56                     | 352,6                | 28,05            | 15,8        | 30,8                                   | 0,96                       |
| 7   | 0,274                      | 0,46                     | 66,4                 | 5,09             | 18,57       | 7,65                                   | 1,03                       |
| 8   | 0,245                      | 0,47                     | 187,4                | 6,54             | 51,3        | 18,64                                  | 0,92                       |
| 9   | 0,245                      | 0,46                     | 182,8                | 4,61             | 51          | 15                                     | 0,93                       |
| 10  | 0,245                      | 0,12                     | 37,7                 | 4,65             | 30,9        | 10,62                                  | 1,07                       |
| 11  | 0,245                      | 0,13                     | 37,7                 | 4,69             | 29          | 9,97                                   | 1,32                       |
| 12  | 0,245                      | 0,12                     | 37,9                 | 4,61             | 31          | 10,5                                   | 1,1                        |
| 13  | 0,245                      | 1,06                     | 165,2                | 4,61             | 23,7        | 8,59                                   | 1,07                       |
| 14  | 0,245                      | 0,87                     | 71,7                 | 4,61             | 12          | 5,85                                   | 1,21                       |
| 15  | 0,245                      | 0,12                     | 37,8                 | 4,79             | 31          | 10,59                                  | 1,08                       |
| 16  | 0,245                      | 2,25                     | 308,2                | 4,62             | 24,2        | 8,31                                   | 1,2                        |
| 17  | 0,245                      | 2,24                     | 307,7                | 4,65             | 24,2        | 7,9                                    | 1,4                        |
| 18  | 0,245                      | 2,24                     | 309,4                | 5,22             | 24,4        | 8,6                                    | 1,05                       |
| 19  | 0,245                      | 0,45                     | 182,8                | 5,21             | 51,9        | 15,6                                   | 0,94                       |
| 20  | 0,245                      | 0,44                     | 182,8                | 6,11             | 52,81       | 17,5                                   | 1,1                        |
| 21  | 0,235                      | 1,29                     | 582,6                | 43               | 71,3        | 56,9                                   | 1,0                        |
| 22  | 0,235                      | 0,98                     | 293,9                | 42,9             | 44,9        | 52                                     | 0,98                       |

The large-diameter model was made from a pipe with an inside diameter  $d = 19$  mm, wall thickness of 0.5 mm, and length of the heated section  $L = 2.85$  m. A rod with an outside diameter  $d_r = 6$  mm was placed in the pipe to measure the temperature profile of the flow. The thermal load was created by electrically heating a coil wound around the outside surface of the pipe. Copper-(copper-iron) thermocouples were used to measure the temperature of the flow at the inlet to the test section and at its outlet, as well as the temperature of the wall on the middle generatrix at a distance  $x/d_e = 90.3$  from the beginning of the heated section. An experimental unit and model were described in [11].

A small-diameter model was made from a pipe with an inside diameter  $d = 1.4$  mm, wall thickness of 0.1 mm, and length of heated section  $L = 545$  mm. The thermal load was created by passing a direct current through the model. The experimental unit was described in [10]. To reduce heat inflow from the outside, the pipe was placed in a horizontal cryostat with shields cooled by liquid nitrogen and helium. The current and transducer leads were thermally stabilized by nitrogen and helium shields with a reverse helium flow. The temperature of the helium flow at the inlet and outlet of the test section was measured with TSG-2 resistance thermometers that were placed in specially designed mixing chamber which ensured a uniform temperature across the flow.

The wall temperature was monitored by KG resistance thermometers (IP AN Ukrainian SSR) installed at a distance  $x/d = 11, 18, 25, 32, 40, 50, 61, 75, 93, 114, 140, 182,$  and  $239$  from the beginning of the heated section. The thermometers were placed in copper clamps which were electrically insulated from the pipe and were fixed on the middle generatrix of the pipe.

The tests were conducted in the range of regime parameters: 1) for the pipe with  $d = 19$  mm,  $P = 0.12-0.28 \cdot 10^6$  N/m<sup>2</sup>,  $T_0 = 4.6-42.9^\circ\text{K}$ ,  $G = 0.12-4.6 \cdot 10^{-3}$  kg/sec,  $q_w = 37-590$  W/m<sup>2</sup>

TABLE 2. Regime Parameters ( $d = 1.4$  mm)

| No. | $10^{-5} P, \text{ N/m}^2$ | $10^3 G, \text{ kg/sec}$ | $q_w, \text{ W/m}^2$ | $T_0, \text{ K}$ | A. SI units |
|-----|----------------------------|--------------------------|----------------------|------------------|-------------|
| 1   | 0,247                      | 0,211                    | 2169                 | 4,56             | 11,4        |
| 2   | 0,245                      | 0,125                    | 2936                 | 4,57             | 23,4        |
| 3   | 0,241                      | 0,120                    | 3774                 | 4,54             | 31,1        |
| 4   | 0,238                      | 0,123                    | 4917                 | 4,55             | 39,7        |
| 5   | 0,245                      | 0,042                    | 3797                 | 4,88             | 72,4        |
| 6   | 0,584                      | 0,082                    | 1548                 | 4,75             | 17,3        |
| 7   | 0,608                      | 0,119                    | 3452                 | 4,85             | 28,6        |
| 8   | 0,618                      | 0,082                    | 3819                 | 4,73             | 42,6        |
| 9   | 0,559                      | 0,0737                   | 4764                 | 4,64             | 57,9        |

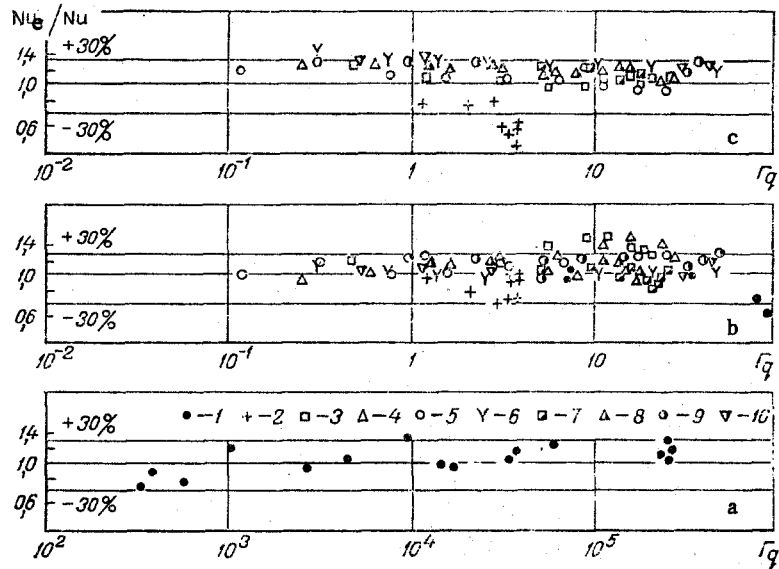


Fig. 1. Comparison of experimental heat-transfer coefficients with theoretical values for forced convection in relation to the thermogravitational-effect parameter  $\Gamma_q$ : a, b)  $Nu$  from Eq. (1); c)  $Nu$  from the equation in [14]; with  $d_e = 18$  mm (1) regimes Nos. 1-22 (Table 1); with  $d = 1.4$  mm (2) regime No. 1; 3) No. 2; 4) No. 3; 5) No. 4; 6) No. 5; 7) No. 6; 8) No. 7; 9) No. 8; 10) No. 9 (Table 2).

(Table 1); 2) for the pipe with  $d = 1.4$  mm,  $P = 0.24-0.62 \cdot 10^6$  N/m<sup>2</sup>,  $T_0 = 4.5-8^\circ\text{K}$ ,  $G = 0.07-0.13 \cdot 10^{-3}$  kg/sec,  $q_w = 950-7300$  W/m<sup>2</sup> (Table 2).

The amount of heat overflow was insignificant (less than 7% of  $q_w$ ) in the investigated wall-temperature range due to the low thermal conductivity of the material.

The helium temperature was both greater and less than the pseudocritical temperature  $T_m$  during the tests. The flow temperature  $T = T_m$  was found at the beginning of the heated section in most of the regimes. This was connected with the relatively high temperature of the flow  $T_0$  at the inlet ( $(T_0)_{\min} = 4.5^\circ\text{K}$ ) and the large thermal loads (A to 70 SI units).

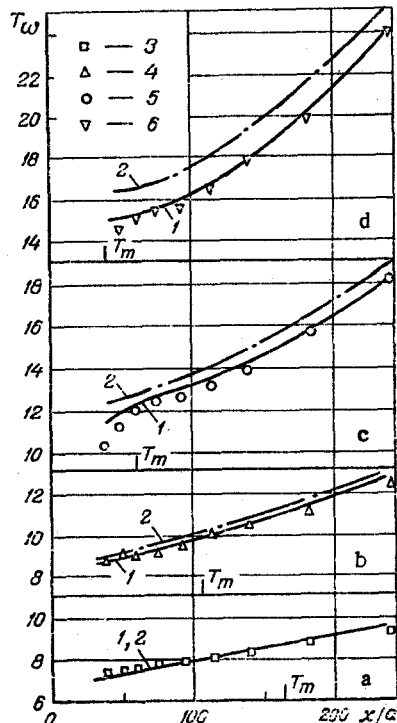


Fig. 2. Change in wall temperature  $T_w$  (K) along the pipe with  $d = 1.4$  mm at  $P = 0.6 \cdot 10^6$  N/m<sup>2</sup>: 1)  $T_w$  from Eq. (1); 2)  $T_w$  from the equation in [14]; 3) regime No. 4; 4) No. 7; 5) No. 8; 6) No. 9 (Table 2).

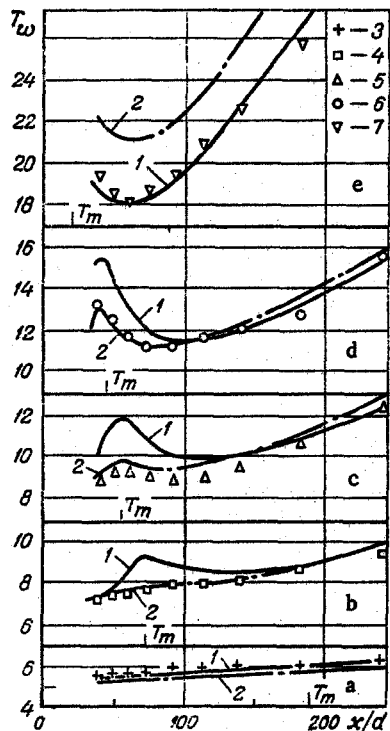


Fig. 3.

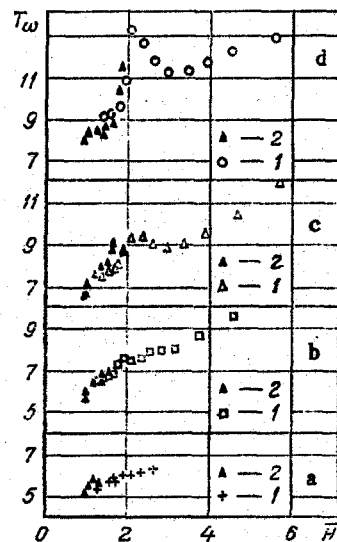


Fig. 4.

Fig. 3. Change in the wall temperature  $T_w$  along the pipe with  $d = 1.4$  mm at  $P = 0.25 \cdot 10^6$  N/m<sup>2</sup>: 1)  $T_w$  from Eq. (1); 2)  $T_w$  from the equation in [14]; 3) regime No. 1; 4) No. 2; 5) No. 3; 6) No. 4; 7) No. 5 (Table 2).

Fig. 4. Profile of wall temperature  $T_w$  (°K) with  $P = 0.15 \cdot 10^6$  N/m<sup>2</sup>: 1) Table 2; 2) data from [4]; a) 1 - regime No. 1; 2 -  $P = 0.253 \cdot 10^6$  N/m<sup>2</sup>;  $G = 0.243 \cdot 10^{-3}$  kg/sec;  $q_w = 1766$  W/m<sup>2</sup>;  $T_o = 4.048$ °K;  $A = 11.3$  SI units;  $d = 2.13$  mm; b) 1 - regime No. 2; 2 -  $P = 0.253 \cdot 10^6$  N/m<sup>2</sup>;  $G = 0.418 \cdot 10^{-3}$  kg/sec;  $q_w = 2535$  W/m<sup>2</sup>;  $T_o = 4.047$ °K;  $A = 22.5$  SI units; c) 1 - regime No. 3; 2 -  $P = 0.253 \cdot 10^6$  N/m<sup>2</sup>;  $G = 0.401 \cdot 10^{-3}$  kg/sec;  $q_w = 4728$  W/m<sup>2</sup>;  $T_o = 4.049$ °K;  $A = 31.6$  SI units; d) 1 - regime No. 4; 2 -  $P = 0.253 \cdot 10^6$  N/m<sup>2</sup>;  $G = 0.423 \cdot 10^{-3}$  kg/sec;  $q_w = 6015$  W/m<sup>2</sup>;  $T_o = 4.053$ °K;  $A = 38.5$  SI units.  $\bar{H}$ ,  $10^{-4}$  J/kg.

It was found that heat transfer on the stabilized section on the middle generatrix of the tube with  $d = 19$  mm was close to the heat transfer in forced convection (Eq. (1)) within a broad range of values of the parameter describing the thermogravitational effect  $\Gamma_q$  (Fig. 1a and b).

Despite the small diameter, the thermogravitational effect should be substantial on the pipe with  $d = 1.4$  mm, since the parameter  $\Gamma_q$  reached 70 in [16]. However, on the middle generatrix of the pipe, as for the pipe with  $d = 19$  mm, heat transfer was the same as in forced convection on the section of stabilized heat transfer with  $P = 0.6 \cdot 10^6$  N/m<sup>2</sup> (Fig. 2a-d). With  $P = 0.25 \cdot 10^6$  N/m<sup>2</sup>, the agreement with the values calculated from Eq. (1) is less satisfactory, particularly near  $T_m$ , beginning with  $A$  greater than 20 SI units (Fig. 3). A comparison made using the correlation relation for forced convection [14] (Fig. 1c) showed better agreement for  $20$  SI units  $< A < 40$  SI units (Fig. 3b, c, and d) and poorer agreement in the regions  $A < 20$  SI units and  $A > 40$  SI units (Fig. 3a and e).

The measurements on the middle generatrix of the horizontal pipe in the range of  $\Gamma_q$  up to 40 agree satisfactorily with the data obtained in [4] (Fig. 4) on vertical pipes with an upward flow of helium when the thermogravitational effect on heat transfer is slight,  $Gr_p/Re^2 < 0.01$ .

Thus, it can be assumed that heat transfer to helium on the middle generatrix of a horizontal pipe with a low-heat-conducting wall in regimes of mixed turbulent convection can be adequately described within a broad range of values of the parameter indicating the thermogravitational effect on heat transfer  $\Gamma_q$  (up to  $10^6$ ) by the correlation relations in [13, 14] for forced turbulent convection.

#### NOTATION

$x$ , distance from the beginning of heating, m;  $d$ , inside diameter of the pipe, m;  $d_e$ , effective diameter of the annular channel, m;  $q_w$ , heat flux,  $W/m^2$ ;  $G$ , mass rate, kg/sec;  $\rho u$ , specific mass rate,  $kg/sec \cdot m^2$ ;  $P$ , pressure,  $N/m^2$ ;  $T_0$ , temperature at the inlet,  $^{\circ}K$ ;  $T_w$ , temperature of the inside surface,  $^{\circ}K$ ;  $\bar{T}$ , mean mass temperature of helium,  $^{\circ}K$ ;  $H_w$ , enthalpy of helium at  $T_w$ ,  $J/kg$ ;  $\bar{H}$ ,  $c_p$ ,  $\rho$ ,  $\mu$ ,  $\lambda$ ,  $\beta$ , enthalpy of flow, specific heat, density, viscosity, thermal conductivity, and coefficient of cubical expansion at  $\bar{T}$ , respectively;  $Nue$ , experimental value of the Nusselt number;  $Nu$ , calculated value of the Nusselt number;  $A = q_w d^{0.2} / (\rho u)^{0.8}$ , parameter of the boundary conditions of the regime, SI units;  $Nu_0 = 0.023 Re^{0.8} Pr^{0.4}$ ;  $Gr_q = \beta \rho^2 d^4 g q_w / \lambda \mu^2$ ;  $Gr_\rho = g \rho^2 (1 - \rho_w / \rho) d^3 / \mu^2$ ;  $\Gamma_q = Gr_q / Gr_L$ , parameter of thermogravitational effect on heat transfer [16];  $Gr_L = 3 \cdot 10^{-5} Re^{2.75} Pr^{0.5} [1 + 2.4 Re^{-0.125} (Pr^{2/3} - 1)]$ , limiting value of the Grashof criterion [15];  $T^* = \bar{T}$  at  $\bar{T} < T_m$ ;  $T^* = T_m$  at  $\bar{T} > T_m$ .

#### LITERATURE CITED

1. P. J. Giarratano, V. D. Arp, and R. V. Smith, "Forced convection heat transfer to supercritical helium," *Cryogenics*, 11, No. 5, 385-393 (1971).
2. H. Odata and S. Sato, "Measurements of forced convection heat transfer to supercritical helium," *Proceedings of the Fourth International Cryogenic Engineering Conference*, Eindhoven, Netherlands, May 24-26 (1972), pp. 291-294.
3. C. Johannes, "Studies of forced convection heat transfer to helium I," *Adv. Cryog. Eng.*, 17, 352-360 (1972).
4. P. J. Giarratano and M. C. Jones, "Deterioration of heat transfer to supercritical helium at 2.5 atm.," *Int. J. Heat Mass Transfer*, 18, 649-653 (1975).
5. V. G. Pron'ko, G. I. Malyshev, and L. N. Migalinskaya, "Regimes of normal and deteriorated heat transfer in the single-phase near-critical region in turbulent helium flow in pipes," *Inzh.-Fiz. Zh.*, 30, No. 4, 606-611 (1976).
6. D. J. Brassington and D. N. H. Cairns, "Measurements of forced convection heat transfer to supercritical helium," *Int. J. Heat Mass Transfer*, 20, No. 3, 207-214 (1977).
7. M. L. Dolgoi and A. M. Troyanov, "Heat transfer in a flow of helium with near-critical parameters in a horizontal channel," in: *Heat and Mass Transfer Processes in Cryogenic Systems* [in Russian], Naukova Dumka, Kiev (1980), pp. 21-26.
8. V. G. Pron'ko, G. P. Malyshev, and I. P. Vishnev, "Heat transfer to supercritical helium in a horizontal channel," in: *Heat and Mass Transfer-VI* [in Russian], A. V. Lykov Institute of Heat and Mass Transfer of the Belorussian Academy of Sciences, Vol. 1, Pt. 1, Minsk (1980), pp. 173-177.
9. M. A. Valyuzhinich, V. M. Eroshenko, E. V. Kuznetsov, and N. N. Yaroslavtseva, "Heat transfer in a helium flow in a forced convection regime at supercritical pressure," in: *Creation of a Superconducting Voltage-Generator Lead* [in Russian], G. M. Krzhizhanovskii Power Engineering Institute, Moscow (1981), pp. 125-132.
10. M. A. Valyuzhinich and E. V. Kuznetsov, "Experimental study of heat transfer in the heating of helium at supercritical pressure," *VINITI*, No. 4708, Sept. 1, 1982.
11. V. M. Jeroshenko, Je. V. Kuznetsov, O. A. Shevchenko, R. C. Hendricks, and D. E. Daney, "Measurements of mixed convective heat transfer to low temperature helium in a horizontal channel," *Proceedings of the Fifteenth International Congress on Refrigeration*, Venice, Italy, Sept. 23-29 (1979), pp. 1-20.
12. R. C. Hendricks, D. E. Daney, V. M. Jeroshenko, Je. V. Kuznetsov, and O. A. Shevchenko, "Some heat transfer and hydrodynamic problems associated with superconducting cables," *Proceedings of the Fifth USA-USSR Symposium on Superconducting Power Transmission*, Brookhaven National Laboratory, Upton, Sept. 5-6, 1978.
13. V. M. Eroshenko and E. V. Kuznetsov, "Calculation of heat transfer and hydraulic resistance in a helium flow in the near-critical thermodynamic state," in: *Superconducting Electrical Power Transmission Lines*, G. M. Krzhizhanovskii Power Engineering Institute, Moscow (1979), pp. 65-74.

14. B. S. Petukhov, A. F. Polyakov, and S. V. Rosnovskii, "New approach to calculating heat transfer with the heat carrier at supercritical pressures," *Teplofiz. Vys. Temp.*, 14, No. 6, 1326-1329 (1976).
15. A. F. Polyakov, "Development of secondary free convection flows in forced turbulent flow in horizontal pipes," *Zh. Prikl. Mekh. Tekh. Fiz.*, No. 5, 60-66 (1974).
16. B. S. Petukhov, A. F. Polyakov, and Yu. L. Shekhter, "Turbulent flow and heat transfer in a gravitational force field," *Teplofiz. Vys. Temp.*, 16, No. 3, 624-639 (1978).

TURBULENT FLOW IN A RECTANGULAR CAVITY IN THE WALL  
OF A TWO-DIMENSIONAL CHANNEL

Ya. I. Kabakov and A. I. Maiorova

UDC 532.517.4

Results are presented of a theoretical and experimental investigation of flow of a turbulent incompressible liquid over a rectangular cavity of relative depth 1-3.

Separated flows of liquid or gas associated with flow over a cavity in a solid wall are encountered in many engineering installations. Such flows have received extensive study, in regard to their external features. Reference [1] has reviewed the experimental investigations of flow of a thick boundary layer over a rectangular cavity in the wall of a wind tunnel. Reference [2] has experimentally studied supersonic gas flow over a cavity in the wall of a two-dimensional channel, with a relative cavity depth to width of from 0.35 to 1.0. Reference [3] has presented results of measurement of the velocity of flow of an incompressible liquid in a square cavity of width equal to four channel heights, at an incident stream Reynolds number of  $\sim 7.5 \cdot 10^3$ . Below we present results of an experimental and theoretical investigation of turbulent flow of an incompressible liquid in rectangular cavities in the wall of a two-dimensional channel for a cavity width equal to the channel height, relative depths of from 1 to 3, and Reynolds numbers from  $10^4$  to  $3.5 \cdot 10^5$ .

1. The turbulent characteristics were measured on an experimental facility, in the form of a channel of square section with side  $H = 0.1$  m, made of clear plastic. The total channel length was 3.5 m. At a distance of 2.5 m from the channel entrance there was a rectangular cavity of extent  $d = H = 0.1$  m, and the depth was varied in the range 0.1-0.3 m. The air entered the experimental facility from the atmosphere through a smooth entrance section, and was drawn in by vacuum pumps. The air velocity on the channel axis was varied from  $U_0 = 17$  to  $U_0 = 60$  m/sec with the help of a slide valve located at a distance of 1 m downstream of the cavity. To measure the velocities and the intensity of turbulence we used a constant-temperature hot-wire anemometer with a frequency characteristic of 30 kHz.

The main bulk of the measurements was made in the central plane of the channel. To determine the nature of the flow, we made control measurements at various longitudinal sections of the cavity. In the test range of Reynolds number, a noticeable breakdown of the two-dimensional flow was observed at distances up to 0.1d from the end walls. Taking into account what was said above, one can consider the flow to be approximately two-dimensional.

2. The method of calculation used in this work is based on numerical integration of the full system of steady-state Reynolds equations [4] for two-dimensional flow of an incompressible fluid:

$$\begin{aligned}
 U \frac{\partial U}{\partial x} + V \frac{\partial U}{\partial y} &= -\frac{\partial P}{\partial x} + \nu \left( \frac{\partial^2 U}{\partial x^2} + \frac{\partial^2 U}{\partial y^2} \right) - \frac{\partial \bar{u}^2}{\partial x} - \frac{\partial \bar{u}v}{\partial y}, \\
 U \frac{\partial V}{\partial x} + V \frac{\partial V}{\partial y} &= -\frac{\partial P}{\partial y} + \nu \left( \frac{\partial^2 V}{\partial x^2} + \frac{\partial^2 V}{\partial y^2} \right) - \frac{\partial \bar{u}v}{\partial x} - \frac{\partial \bar{v}^2}{\partial y}, \\
 \frac{\partial U}{\partial x} + \frac{\partial V}{\partial y} &= 0.
 \end{aligned}
 \tag{1}$$